s and p orbitals, which are altered by the change in Cr–O bond lengths. The term "direct exchange" for J_a is misleading in this respect. We should also realize that a change of only 0.01 Å in the Cr–Cr separation can result in a 10% change of J_a and J. This is the result of recent experiments with $[9](ClO_4)_3$ under hydrostatic pressure.[16] A difference of 0.01 Å in the Cr–Cr separation between $[9](ClO_4)_3$ and $[12]Br_3{\cdot}2H_2O$ cannot be ruled out on the basis of the X-ray diffraction results. It may account for part of the observed difference in J.

Acknowledgment. We acknowledge financial support of this work by the Swiss National Science Foundation.

Registry No. $[12]Br_3{\cdot}2H_2O$, 109306-30-1.

(16) Riesen, H.; Güdel, H. U., submitted for publication in *J. Chem. Phys.*

Contribution from the Istituto di Teoria e Struttura Elettronica, CNR, 00016 Monterotondo Scalo (Roma), Italy, and Institut für anorganische Chemie, Universität Bern, CH-3000 Bern 9, Switzerland

Optical Spectroscopy of One- and Two-Dimensional Ionic Magnets of Cr^{2+}: $CsCrCl_3$, $(CH_3)_4NCrCl_3$, $(CH_3)_4NCrBr_3$, $CrCl_2$, $(C_2H_5NH_3)_2CrCl_4$, and $(C_2H_5NH_3)_2CrBr_4$

Carlo Bellitto,[†] Hans Brunner,[‡] and Hans U. Güdel*[‡]

Received March 5, 1987

The title compounds were synthesized and grown as single crystals. Absorption spectra were measured between 10 and 300 K in the visible and near-infrared range. Spin-allowed transitions were assigned to the near-IR bands. The linear-chain compounds $ACrX_3$ ($A = Rb^+$, Cs^+, $(CH_3)_4N^+$; $X = Cl^-$, Br^-) and $CrCl_2$ show a large number of sharp spin-forbidden bands between 16 000 and 24 000 cm^{-1}, whereas the layer compounds A_2CrX_4 ($A = Rb^+$, Cs^+, $C_nH_{2n+1}NH_3^+$; $X = Cl^-$, Br^-) show only two band systems around 16 000 and 19 000 cm^{-1}. This difference is interpreted in terms of an exchange intensity mechanism, and the bands observed near 16 000 and 19 000 cm^{-1} are assigned as $^5B_{1g} \rightarrow {}^3B_{1g}(^3H)$ and $^3B_{1g}(^3F)$ transitions. The small number of spin-forbidden bands in A_2CrX_4 is due to a lack of orbital overlap between the magnetic orbitals on nearest-neighbor Cr^{2+} ions. It is thus correlated to the observed ferromagnetic ground state in these compounds. In contrast, the crystal structures of $ACrX_3$ and $CrCl_2$ are more favorable for orbital overlap. As a consequence, these compounds are antiferromagnets and exhibit a larger number of spin-forbidden excitations within the ground-state electron configuration.

1. Introduction

Ternary chromium(II) halides of the general composition $ACrX_3$ ($A = Rb^+$, Cs^+, $(CH_3)_4N^+$; $X = Cl^-$, Br^-) crystallize in structures derived from the well-known hexagonal $CsNiCl_3$ structure.[1-4] Since Cr^{2+} is subject to $E \otimes e$ Jahn–Teller distortions, the local coordination geometry is approximately D_{4h}. Structural phase transitions resulting from a cooperative Jahn–Teller effect have been observed and investigated in $RbCrCl_3$, $CsCrCl_3$, $CsCrBr_3$, and $(CH_3)_4NCrCl_3$.[1] In the high-temperature phase the directions of the elongated Cr–Cl bonds are considered to be disordered along the chains, thus retaining the overall hexagonal symmetry of the $CsNiCl_3$ structure. The low-temperature phases correspond to superstructures with ordered directions of the elongated Cr–Cl bonds and correspondingly lower symmetry space groups. The magnetic and caloric properties of $ACrX_3$ compounds show typical features of one-dimensional antiferromagnets.[2-5] $(CH_3)_4NCrCl_3$ (TMCC) shows a transition to three-dimensional magnetic order at 7 K.[2] In this respect it resembles $(CH_3)_4NMnCl_3$ (TMMC), the prototypical one-dimensional antiferromagnet.

Detailed single-crystal optical spectra have been reported for $RbCrCl_3$ and $CsCrCl_3$ as well as their diluted analogues $RbMg_{1-x}Cr_xCl_3$ and $CsMg_{1-x}Cr_xCl_3$.[1,6-8] Some authors have assumed local O_h symmetry in the assignment of the spin-allowed absorption bands, while other analyses are based on the more realistic assumption of a local D_{4h} distortion.[1,8] Spin-forbidden bands have only been interpreted in O_h.

$CrCl_2$ has a chain structure with edge-sharing octahedra along the c axis of the orthorhombic unit cell.[9] The elongated Cr–Cl bonds are not involved in the bridging between nearest-neighbor Cr^{2+} ions in the chains.[10] A transition to three-dimensional antiferromagnetic order was observed at 20 K. Unpolarized single-crystal absorption spectra in the near-infrared and visible region have been reported and interpreted.[11]

Ternary chromium(II) halides of the composition A_2CrX_4 ($A = Rb^+$, Cs^+, RNH_3^+; $X = Cl^-$) crystallize in a distorted K_2NiF_4 layer structure. Recently several A_2CrBr_4 compounds ($A = C_2H_{2n+1}NH_3^+$) have been synthetsized and characterized.[12,13] They are all two-dimensional ferromagnets. As a result of the ferromagnetic exchange coupling within the layers they exhibit very interesting and quite unique physical properties at low temperatures. Their structural, magnetic, and spectroscopic properties have therefore been studied in much more detail than for the corresponding CrX_2 and $ACrX_3$ compounds.[14] Optical spectroscopists have focused on two absorption band systems, which show a very distinct temperature dependence typical of two-dimensional ferromagnets.

The visible part of the absorption spectrum of Cr^{2+} with chloro or bromo coordination consists of spin-forbidden transitions. The

[†] CNR Rome.
[‡] Universität Bern.

(1) Crama, W. J. Ph.D. Thesis, Rijksuniversiteit Leiden, 1980.
(2) Bellitto, C.; Dessy, G.; Fares, V.; Fiorani, D.; Viticoli, S. *J. Phys. Chem. Solids* **1984**, *45*, 1129.
(3) Bellitto, C.; Fiorani, D.; Viticoli, S. *Inorg. Chem.* **1985**, *24*, 1939.
(4) Ackermann, J.; Cole, G. M.; Holt, S. L. *Inorg. Chim. Acta* **1974**, *8*, 323.
(5) Hatfield, W. E.; Estes, W. E.; Marsh, W. E.; Pickens, M. W.; ter Haar, L. W.; Weller, R. R. In *Extended Linear Chain Compounds*; Miller, J. S., Ed.; Plenum: New York, 1983; Vol. 3, p 43.
(6) McPherson, G. L.; Kistenmacher, T. J.; Folkers, J. B.; Stucky, G. D. *J. Chem. Phys.* **1972**, *57*, 3771.
(7) Alcock, N. W.; Putnik, C. F.; Holt, S. L. *Inorg. Chem.* **1976**, *15*, 3175.
(8) Reinen, D.; Friebel, C. *Struct. Bonding (Berlin)* **1979**, *37*, 1.
(9) Tracy, J. W.; Gregory, N. W.; Lingafelter, E. C.; Dunitz, J. D.; Mez, H.-C.; Rundle, R. E.; Scheringer, C.; Yakel, H. L.; Wilkinson, M. K. *Acta Crystallogr.* **1961**, *14*, 927.
(10) Cable, J. W.; Wilkinson, M. K.; Wollan, E. O. *Phys. Rev.* **1960**, *118*, 950.
(11) Rosseinsky, D. R.; Dorrity, I. A. *J. Phys. Chem.* **1977**, *81*, 2672.
(12) Babar, M. A.; Larkworthy, L. F.; Yavari, A. *J. Chem. Soc., Dalton Trans.* **1981**, 27.
(13) Bellitto, C.; Filaci, P.; Patrizio, S. *Inorg. Chem* **1987**, *26*, 191.
(14) Day, P. *J. Magn. Magn. Mater.* **1986**, *54–57*, 1442.
(15) Janke, E.; Wood, T. E.; Ironside, C.; Day, P. *J. Phys. C* **1982**, *15*, 3809.

0020-1669/87/1326-2750$01.50/0

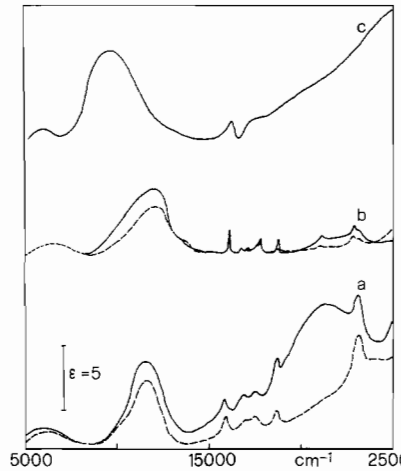

Figure 1. Polarized near-IR and visible crystal absorption spectra at 14 K of (a) $CsCrCl_3$ and (b) $(CH_3)_4NCrCl_3$ ($\vec{E} \parallel \vec{c}$ (—) and $\vec{E} \perp \vec{c}$ (---)). The line (c) corresponds to a diffuse-reflectance spectrum of $(CH_3)_4NCrBr_3$ at 298 K.

observed spectra of $ACrX_3$ and $CrCl_2$ on the one hand and A_2CrX_4 on the other are strikingly different. Whereas the former show a large number of sharp bands covering the range from 16 000 to 24 000 cm^{-1}, there are only two intense band systems at approximately 16 000 and 19 000 cm^{-1} in the latter. The reason for this distinctly different behavior in the spin-forbidden spectral region is not understood, and it has not previously been investigated. It is one of the aims of the present paper to shed some light on this question. We present polarized single-crystal absorption spectra of the title compounds in section 3. A detailed analysis of the intensity mechanism for spin-forbidden transitions follows in section 4. A correlation between spectroscopic and structural properties is established, which explains the different visible spectra of the various structure types.

2. Experimental Section

All the Cr^{2+} compounds are hygroscopic and are very easily oxidized. The synthesis and the handling of materials were therefore carried out under inert atmosphere or under vacuum.[16]

$(CH_3)_4NCrX_3$ (X = Cl^- (TMCC), Br^- (TMCB)) were synthesized according to previously reported procedures.[2,3] Single crystals suitable for optical spectroscopy were obtained by slow addition of a solution of the corresponding tetramethylammonium salt to the Cr^{2+} solution. In the case of $(CH_3)_4NCrCl_3$ better crystals were obtained by slow interdiffusion of anhydrous ethanol solutions of $CrCl_2$ and $(CH_3)_4NCl$ through a porous set under an inert atmosphere.

$(C_2H_5NH_3)_2CrCl_4$ was synthesized by a previously reported procedure.[18] $(C_2H_5NH_3)_2CrBr_4$ was synthesized by following the procedure described recently for $(C_6H_5CH_2NH_3)_2CrBr_4$.[13]

Single crystals of $CrCl_2$ and $CsCrCl_3$ were prepared by the Bridgman technique. The chain axes could be identified from the observed cleavage properties.

All the compounds were characterized by X-ray powder diffraction, and the purity was further checked by the absence of typical Cr^{3+} bands centered at about 600 and 450 nm in the optical spectrum.

For $CsCrCl_3$ thin slices with faces containing the c axis, which were suitable for optical spectroscopy, were obtained by using a polishing machine. Freshly cleaved faces were used with $CrCl_2$. The compounds $(CH_3)_4NCrCl_3$, $(C_2H_5NH_3)_2CrCl_4$, and $(C_2H_5NH_3)_2CrBr_4$ had well-developed growth faces, which were directly used for spectroscopy. The bromides are extremely air-sensitive, and TMCB could only be obtained in the form of microcrystals.

Polarized absorption spectra were recorded on a Cary 17 spectrophotometer equipped with a pair of Glan-Taylor prisms and a GaAs photocathode for better sensitivity in the range 700–900 nm. The samples were cooled with a Displex closed-cycle cryostat (Air Products) or a helium gas-flow tube. Diffuse-reflectance spectra were measured on a Beckman DK-2A spectrophotometer with MgO as a reference.

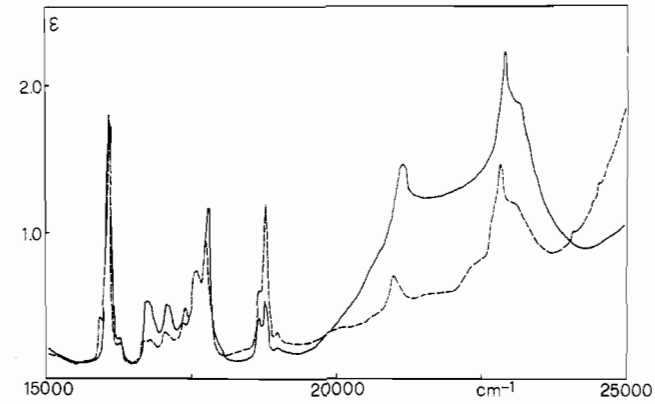

Figure 2. Section of the polarized visible crystal absorption spectrum at 14 K of $(CH_3)_4NCrCl_3$: (—) $\vec{E} \parallel \vec{c}$; (---) $\vec{E} \perp \vec{c}$.

3. Results

Figure 1 shows polarized 14 K absorption spectra of $CsCrCl_3$ and TMCC in the near-infrared and visible regions. They are supplemented by a 298 K powder reflectance spectrum of TMCB. The prominent broad and asymmetric absorption band centered at approximately 11 500 cm^{-1} in the chlorides is readily assigned to a spin-allowed transition. It has the typical temperature dependence of a vibronically induced transition. In the following we use D_{4h} notation for the designation of states, and in parentheses we give the octahedral parentage. The two overlapping bands are thus assigned to the transitions $^5B_{1g}(E_g) \rightarrow {}^5B_{2g}(T_{2g})$ and $^5E_g(T_{2g})$. Their energy difference corresponds to the splitting of the octahedral $^5T_{2g}$ state as a result of the local Jahn-Teller distortion. The lowest energy absorption band at approximately 6200 cm^{-1} in $CsCrCl_3$ can unambiguously be assigned as $^5B_{1g}(E_g) \rightarrow {}^5A_{1g}(E_g)$ on the basis of its temperature dependence and absolute intensity. It is vibronically induced like the 11 500-cm^{-1} band and unlike the sharp bands in the visible region. The position of the $^5B_{1g} \rightarrow {}^5A_{1g}$ band shows some variation between the various chloro compounds. The following low-temperature values can be estimated: 6400 cm^{-1} for TMCC, 9100 cm^{-1} for $CrCl_2$,[11] and 7000 cm^{-1} for Rb_2CrCl_4.[17] This is a reflection of slight differences in the tetragonal crystal field and electron repulsion parameters. In particular, we notice a significantly higher energy of this band in $CrCl_2$. This can be correlated with structural data. In $CrCl_2$ the axial elongation of the $CrCl_6$ unit is 0.52 Å,[9,10] compared to 0.32 and 0.20 Å in Rb_2CrCl_4[8] and γ-$CsCrCl_3$,[1] respectively.

There is an additional broad band centered at approximately 22 000 cm^{-1} in $CsCrCl_3$ and TMCC. Its intensity relative to that of the 11 500-cm^{-1} band is much higher in $CsCrCl_3$ than in TMCC. It is completely π-polarized, and its intensity is temperature-independent within experimental accuracy. It has been assigned as a double excitation on the basis of its energy as well as its concentration dependence in $CsMg_{1-x}Cr_xCl_3$.[6] If an impurity origin is ruled out, one is clearly forced to this assignment, even though the mechanism by which the transition can gain intensity is by no means clear. The fact that the transition is so much weaker in TMCC than in $CsCrCl_3$ indicates a mechanism that depends very strongly on the Cr–Cr distance between the nearest neighbors in the chain. The dependence must be stronger than for the usual exchange mechanism responsible for the spin-forbidden bands (section 4). Cr–Cr distances in $CsCrCl_3$ and TMCC are 3.12 and 3.26 Å, respectively. There is no indication for the presence of such a band in the spectra of $CrCl_2$, $(C_2H_5NH_3)_2CrCl_4$, and $(C_2H_5NH_3)_2CrBr_4$.

Figure 2 shows the visible part of the polarized low-temperature absorption spectrum of TMCC. It is highly structured with band widths considerably narrower than in the $CsCrCl_3$ spectrum.[6] Some of the bands have distinct polarization properties. The band intensities in this region are temperature-independent within experimental accuracy between 10 and 300 K. The bands are

(16) Shriver, D. F. *The Manipulation of Air-Sensitive Compounds*; McGraw-Hill: New York, 1969.
(17) Estimated from the room-temperature data in: Münninghoff, G.; Treutmann, W.; Hellner, E.; Heger, G.; Reinen, D. *J. Solid State Chem.* **1980**, *34*, 289.
(18) Bellitto, C.; Day, P. *J. Chem. Soc., Dalton Trans.* **1978**, 1207.

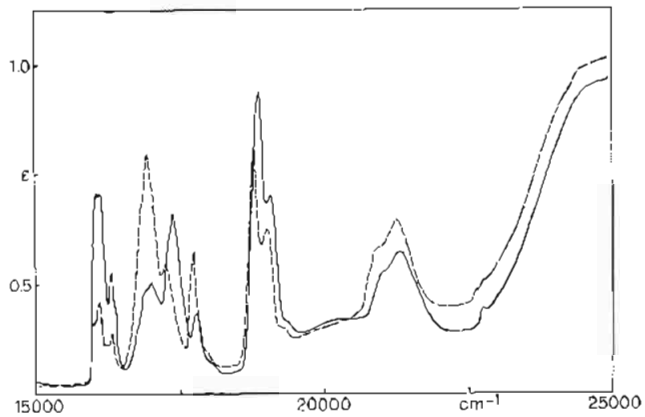

Figure 3. Section of the polarized visible crystal absorption spectrum at 14 K of $CrCl_2$: (—) $\vec{E} \perp \vec{c}$; (---) $\vec{E} \parallel \vec{c}$.

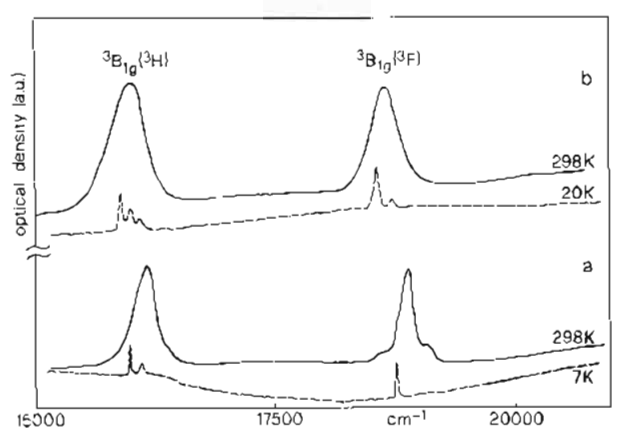

Figure 4. Section of the visible crystal absorption spectra of (a) $(C_2H_5NH_3)_2CrCl_4$ and (b) $(C_2H_5NH_3)_2CrBr_4$ and assignment of spin-forbidden bands. The spectra were measured unpolarized with the light propagating perpendicular to the well-developed plates. The 7 K spectrum of $(C_2H_5NH_3)_2CrCl_4$ is an uncorrected single-beam transmission spectrum.

readily assigned to spin-forbidden d–d excitations, of which a large number are expected on the basis of a Tanabe–Sugano diagram in this spectral range. Assignments of individual bands are rather tricky. In section 4 we will present a comparative discussion of intensity mechanisms for the three structure types studied here, which will enable us to make a partial assignment.

Figure 3 shows the same spectral region for $CsCl_2$ at 14 K. As in TMCC and $CsCrCl_3$, there is a large number of sharp bands between 16000 and 22000 cm^{-1}, covering approximately the same spectral range. Some bands are very strongly polarized. The temperature dependence of some unpolarized absorption bands in this spectral range has been reported and correlated with the antiferromagnetic ordering at 20 K.[11] Our polarized spectra are in agreement with the trends reported in ref 11.

Figure 4 shows high- and low-temperature absorption spectra of $(C_2H_5NH_3)_2CrX_4$ ($X = Cl^-, Br^-$) in the same spectral region. The spectra were measured with unpolarized light propagating perpendicular to the well-developed faces of the plates. The observed behavior is typical of compounds with the composition A_2CrX_4 ($A = Rb^+, Cs^+, RNH_3^+$; $X = Cl^-, Br^-$) crystallizing in distorted K_2NiF_4 layer structures. In contrast to the case for TMCC and $CrCl_2$ (Figures 2 and 3) there are only two band systems between 16000 and 22000 cm^{-1}. At low temperature they are centered at approximately 16000 and 18800 cm^{-1} in the chloride and at about 16000 and 18600 cm^{-1} in the bromide. They show typical hot band behavior, with the intensity increasing approximately proportional to T^2 at low temperatures. This behavior has been investigated in detail for other A_2CrX_4 compounds and interpreted in terms of the two-dimensional magnetic structure. In Rb_2CrCl_4 the two bands were shown to be predominantly polarized within the layers.[15]

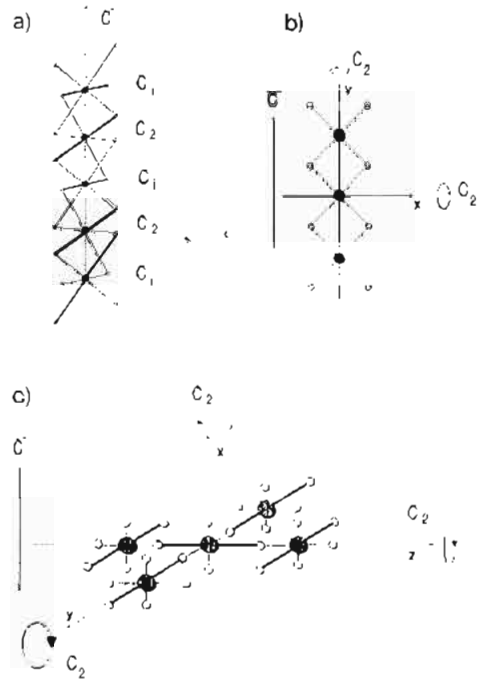

Figure 5. Schematic diagrams of the relevant structure elements of (a) α-$CsCrCl_3$ and TMCC, (b) $CrCl_2$, and (c) A_2CrX_4 ($A = Rb^+, Cs^+, RNH_3^+$; $X = Cl^-, Br^-$). The long axes of the elongated $CrCl_6^{4-}$ octahedra are drawn as thick lines.

4. Discussion of Spin-Forbidden Excitations

We follow ref 1 and assume a D_{4h} distortion resulting from Jahn–Teller interactions at the Cr^{2+} sites in all the compounds. Further smaller distortions are induced by the crystal structures, so that the actual point symmetry is lower than D_{4h} in each case. For an analysis of intensity mechanisms we need to consider the bridging arrangements between nearest and second-nearest Cr^{2+} neighbors in the lattice. This is shown in Figure 5 for the three relevant lattice types.

Below 171 K $CsCrCl_3$ adopts the γ-$CsCrCl_3$ structure with an ordered sequence of the elongated Cr–Cl directions along the chain. There are three inequivalent Cr^{2+} sites in this structure. Two of these are very similar, and Figure 5a shows this idealized structure with Cr^{2+} ions on alternative C_i and C_2 sites along the chain. Following Crama,[1] we assume that TMCC adopts the same structure below the structural phase transition at 230 K. In $CrCl_2$ (Figure 5b) the bridging between neighboring Cr^{2+} ions only involves short Cr–Cl bonds. The elongated Cr–Cl bonds are all perpendicular to the chain axes, thus connecting neighboring chains. In the A_2CrX_4 structure (Figure 5c) long and short Cr–Cl bonds alternate within the layers, leading to the typical antiferrodistorted structure. The Cr–Cl bonds perpendicular to the layers are all short.

Spin-forbidden excitations in magnetically coupled systems can acquire intensity through an exchange mechanism. Tanabe and Ebara have applied this formalism to exchange-coupled chains and derived expressions for the temperature dependence of the spin-forbidden excitations.[19,20] They have also shown how selection rules can be derived, and this is what we will concentrate on. The relevant chain segment to be considered contains three magnetic ions. In the idealized γ-$CsCrCl_3$ structure (Figure 5a) there are two types of such clusters with C_i and C_2 point symmetry, respectively. The $C_2 = z$ axis in the C_2 cluster lies perpendicular to the chain axis. In $CrCl_2$ the relevant chain segment containing three Cr^{2+} ions has D_{2h} symmetry. We use the same principle for A_2CrX_4, thus extending the formalism from one-dimensional to a two-dimensional system. The cluster shown in Figure 5c, including all the nearest neighbors of a given Cr^{2+} ion and thus

(19) Tanabe, Y.; Ebara, K. *J. Phys. Soc. Jpn.* **1971**, *30*, 886.
(20) Ebara, K.; Tanabe, Y. *J. Phys. Soc. Jpn.* **1974**, *36*, 93.

Table I. Selection Rules for Exchange-Induced Spin-Forbidden Transitions[a]

γ-$CsCrCl_3$

excited state	$\vec{E} \parallel$ chain	$\vec{E} \perp$ chain	excited state	$\vec{E} \parallel$ chain	$\vec{E} \perp$ chain
$^3A_{1g}$	–	+	$^3B_{2g}$	–	+
$^3A_{2g}$	+	+	$^3E_{g(xz)}$	–	+
$^3B_{1g}$	+	+	$^3E_{g(yz)}$	+	+

$CrCl_2$

excited state	$\vec{E} \parallel$ chain (c) axis	$\vec{E} \perp$ chain (c) axis	excited state	$\vec{E} \parallel$ chain (c) axis	$\vec{E} \perp$ chain (c) axis
$^3A_{1g}$	–	+	$^3B_{2g}$	–	+
$^3A_{2g}$	+	–	$^3E_{g(xz)}$	–	–
$^3B_{1g}$	+	–	$^3E_{g(yz)}$	–	+

A_2CrX_4

excited state	$\vec{E} \perp$ layer	$\vec{E}$ within layer	excited state	$\vec{E} \perp$ layer	$\vec{E}$ within layer
$^3A_{1g}$	–	+	$^3B_{2g}$	+	–
$^3A_{2g}$	+	–	$^3E_{g(xz)}$	+	–
$^3B_{1g}$	–	+	$^3E_{g(yz)}$	–	+

[a] All notations are in D_{4h}. The ground state is $^5B_{1g}$.

containing five Cr^{2+} ions, is considered to be the relevant layer segment. The cluster symmetry is D_{2h}. The coordinate systems used are included in Figure 5b,c. The selection rules for spin-forbidden transitions in these clusters can now be derived by using the procedure of ref 19. In a final step these cluster selection rules are transformed to crystal selection rules, which are then directly comparable with experimental results. Table I gives a summary of the crystal selection rules. For γ-$CsCrCl_3$ the selection rules given in Table I are based on the C_2 cluster. For the C_i cluster all the transitions are allowed. We thus suspect a superposition of both types of intensities in the actual spectrum.

Having dealt with the symmetry aspect of the exchange intensity mechanism, we now turn to a brief discussion of the orbital contributions to this intensity. According to Tanabe and Gondaira, the dominant terms in the intensity expression will be those that can be related to a one-electron transfer between neighboring Cr^{2+} ions.[21] In other words, we have to examine how the orbitals of a given Cr^{2+} center can overlap with the orbitals of its nearest neighbors, thus providing a pathway for exchange-induced intensity. This is of particular interest for the compounds A_2CrX_4. On the basis of Table I alone we would certainly not expect a much smaller number of spin-forbidden bands in $(C_2H_5NH_3)_2CrCl_4$ than in $CrCl_2$. Yet this is what we observe, and we suspect that in the layer compounds some of the orbital pathways for gaining intensity are blocked by the lack of overlap between d orbitals on nearest neighbors.

Figure 6 shows the relative disposition of tetragonal d orbitals on neighboring Cr^{2+} ions in A_2CrX_4. There is a dominant σ overlap between the z^2 orbital of a given Cr^{2+} ion and the $x^2 - y^2$ orbital on its nearest neighbor, which involves a p(σ) orbital on the intervening halide ion. Since z^2 is singly occupied and $x^2 - y^2$ unoccupied, this is thought to be mainly responsible for the ferromagnetic nature of the coupling within the layers in this type of structure.[8] All the overlaps between singly occupied orbitals are either zero by symmetry or are small. The two nonvanishing π overlaps involving p(π) orbitals on the intervening halide ion, yz–yz and xz–xy, must be much smaller than the above-mentioned z^2–$(x^2 - y^2)$ σ overlap. They contribute to the (antiferromagnetic) kineic exchange, but this contribution is obviously too small to override the ferromagnetic effect from the σ overlap.

We follow the reasoning of ref 21 and assume that the dominant orbital terms for exchange-induced intensity correspond to the dominant pathways for exchange. In the A_2CrX_4 structures the singly occupied z^2 orbital plays the central role in this respect.

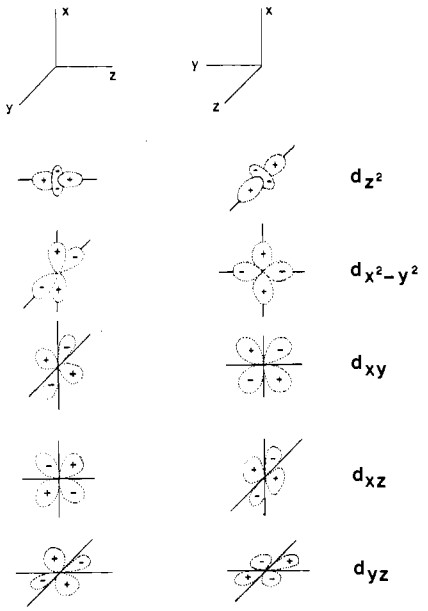

Figure 6. Relative orientation of d orbitals on neighboring Cr^{2+} ions in A_2CrX_4. z is the axis of elongation of the $CrCl_6^{4-}$ octahedron.

Flipping the spin of the electron in this orbital, thus creating a triplet state, corresponds to an electronic excitation, the intensity of which is most strongly enhanced by the exchange mechanism. We therefore have to investigate which triplet excited states are derived from such a spin flip. The strong-field wave function for the ground state of Cr^{2+} in a tetragonal ligand field is given by

$$^5B_{1g}(M_s = 2) = |z^2\ xy\ xz\ yz| \quad (1)$$

The configuration ($\bar{z}^2\ xy\ xz\ yz$) contributes to the following triplet functions:[22]

$$\bar{z}^2\ xy\ (^3B_{2g})\ xz\ yz\ (^3A_{2g}) \qquad ^3B_{1g}(M_s = 1) \quad (2)$$

$$\bar{z}^2\ xy\ (^1B_{2g})\ xz\ yz\ (^3A_{2g}) \qquad ^3B_{1g}(M_s = 1) \quad (3)$$

Using pages 175 and 177 of ref 22, we can now identify those excited states whose wave functions have dominant contributions from the functions(2) and (3): $^3B_{1g}(^3H)$ expected at approximately 16 500 cm^{-1} and $^3B_{1g}(^3F)$ expected at approximately 20 500 cm^{-1}. In the crystal field calculations of ref 22 the Racah formalism was used. This is known to be quite inadequate even for the free Cr^{2+} ion energies.[11] In particular, the crystal field terms deriving from ^3F are overestimated by up to 2000 cm^{-1}. We therefore feel confident in assigning the typical and prominent band systems centered near 16 000 and 19 000 cm^{-1} in the A_2CrX_4 spectra to the $^3B_{1g}(^3H)$ and $^3B_{1g}(^3F)$ excitations. This is in agreement with ref 15, where the same assignment was proposed without using intensity arguments. Our emphasis here is on the absence of any other bands in the visible region of the A_2CrX_4 spectra, which is very nicely accounted for by the above argumentation.

For $CrCl_2$ we can use similar arguments. The relevant magnetic orbitals in this structure are those that can promote an electron transfer between neighboring Cr^{2+} centers. Using the coordinate system of Figure 5, we find that xy orbitals can overlap within the plane of the ribbon, whereas xy and yz orbitals have an out-of-plane overlap by way of p_z orbitals on the intervening chloride ions.

Spin flips in the three orbitals xy, xz, and yz are thus the primary candidates for exchange-induced intensity. We therefore have to find the triplet excited states with dominant contributions from the following electron configurations: ($z^2\ \overline{xy}\ xz\ yz$), ($z^2\ xy\ \overline{xz}\ yz$), and ($z^2\ xy\ xz\ \overline{yz}$). Using pages 175 and 177 of ref 22, we find the following: $^3B_{1g}(^3H)$ expected at approximately 16 500

(21) Tanabe, Y.; Gondaira, K. *J. Phys. Soc. Jpn.* **1967**, *22*, 573.

(22) König, E.; Kremer, S. *Ligand Field Energy Diagrams*; Plenum: New York, 1977.

cm^{-1}, $^3A_{2g}(^3G)$ expected at approximately 18 000 cm^{-1}, $^3A_{1g}(^3H)$ expected at approximately 18 500 cm^{-1}, $^3B_{1g}(^3F)$ expected at approximately 20 500 cm^{-1}, and $^3B_{2g}(^3D)$ expected above 22 000 cm^{-1}. Besides the two $^3B_{1g}$ excitations dominating the A_2CrX_4 spectrum, there are two additional transitions in the 16 000–20 000-cm^{-1} energy range that are expected to gain intensity by the Tanabe mechanism. This is in very nice agreement with the observed richness of the absorption spectrum in this spectral range. The sharpness of the absorption bands clearly identifies them as intraconfigurational transitions. The band system just above 16 000 cm^{-1} in the spectrum of $CrCl_2$ has the wrong polarization to be assigned to $^3B_{1g}$. The band near 17 000 cm^{-1}, with predominant polarization parallel to the chain axis, is a much more likely candidate for the $^3B_{1g}(^3H)$ excitation. We attribute this shift of the $^3B_{1g}(^3H)$ energy to the larger tetragonal crystal field and slightly larger electron repulsion parameters in $CrCl_2$. This is also reflected in the significantly higher energy of the $^5A_{1g}(E_g)$ transition compared to that of TMCC and $(C_2H_5NH_3)_2CrCl_4$ (section 3).

The visible spectra of TMCC and $CsCrCl_3$ are similar in appearance to that of $CrCl_2$. A detailed analysis in terms of intensity-gaining orbital mechanisms is complicated by the crystal structure. It is evident, from Figure 5, however, that overlap and thus electron-transfer pathways do exist between neighboring Cr^{2+} ions in the chains. The situation is therefore comparable to that for $CrCl_2$, and the exchange mechanism provides intensity for several transitions in the 16 000–22 000-cm^{-1} range. The polarizations of the bands centered near 16 000 and 19 000 cm^{-1} are compatible with $^3B_{1g}$ excitations, and by analogy with the A_2CrCl_4 spectra we assign them accordingly. The 19 000-cm^{-1} band is possibly a superposition of $^3B_{1g}(^3F)$ and $^3A_{1g}(^3H)$. It therefore appears that the two $^3B_{1g}$ transitions have very similar energies in TMCC and $(C_2H_5NH_3)_2CrCl_4$. This is in good agreement with our conclusion from the $^5A_{1g}(E_g)$ band that the tetragonal crystal field and the electron repulsion parameters are very similar in these compounds. In all our compounds the actual point symmetry at the Cr^{2+} sites is lower than D_{4h}. This, together with spin–orbit coupling, leads to additional splittings and thus increases the number of observed transitions. A fit of calculated crystal field energies to the experimental band positions is not meaningful. The observed strong polarization of some of the bands in the $ACrX_3$ and $CrCl_2$ spectra restricts the possible excited states, but we feel that assignments of all the individual bands would be hazardous.

The striking observation, however, that the $ACrX_3$ and $CrCl_2$ spectra are much richer than the A_2CrX_4 spectra in the range 16 000–22 000 cm^{-1} can now be understood. It is due to the lack of overlap between magnetic orbitals on neighboring Cr^{2+} ions in A_2CrX_4, as discussed above. In $ACrX_3$ and $CrCl_2$, on the other hand, the relative dispositions of magnetic orbitals on neighboring Cr^{2+} ions is more favorable for overlap. This is a direct result of the crystal structures, the bridging geometry between nearest neighbors, in particular. These pathways lead to antiferromagnetic kinetic exchange on the one hand and to exchange-induced intensity for spin-forbidden excitations on the other. Spin flips in the relevant orbitals lead to several excited states that are spectroscopically accessible. It is thus clear that the ferromagnetism and the small number of spin-forbidden bands in the compounds A_2CrX_4 have a common origin: lack of overlap between singly occupied orbitals on neighboring Cr^{2+} ions.

Acknowledgment. We thank S. Patrizio for technical assistance. This work was financially supported by the Consiglio Nazionale delle Ricerche and the Swiss National Science Foundation.

Registry No. $(CH_3)_4NCrBr_3$, 29794-92-1; $(CH_3)_4NCrCl_3$, 29794-88-5; $CsCrCl_3$, 13820-84-3; $CrCl_2$, 10049-05-5; $(C_2H_5NH_3)_2CrCl_4$, 62212-04-8; $(C_2H_5NH_3)_2CrBr_4$, 63949-50-8.

Contribution from the Department of Chemistry, North Carolina State University, Raleigh, North Carolina 27695-8204

Spectroelectrochemical Properties of Ruthenium(II) Tris Chelate Complexes of 2,2′-Bipyrimidine and 2,2′-Bipyrazine

C. D. Tait, R. J. Donohoe,† M. K. DeArmond, and D. W. Wertz*

Received February 18, 1987

The electronic absorption and resonance Raman (RR) spectra of the reduction products of $[Ru(bpm)_3]^{2-n}$ and mixed-ligand complexes $[Ru(bpz)_x(bpy)_{3-x}]^{2-n}$ ($x = 1-3$, $n = 0-3$) are discussed, as well as the low-temperature electron spin resonance (ESR) spectrum of $[Ru(bpz)_3]^0$ (bpm = 2,2′-bipyrimidine, bpz = 2,2′-bipyrazine, and bpy = 2,2′-bipyridine). The ultraviolet (UV) absorption and RR spectra for the reduction products of the tris(bipyrimidine) complex are analogous to those of the tris(bipyridine) complex and argue strongly for a localized redox orbital description. While the ESR and near-IR (near-infrared) absorption spectra also argue for localized redox orbitals in the bpz complexes, the simple $(bpz)_{3-n}/(bpz^-)_n$ $\pi \rightarrow \pi^*$ chromophoric behavior typical in the UV absorption spectrum is not observed. Furthermore, there is a gradual shifting of the RR peaks as electrons are added, with no distinct vibrational pattern from reduced and unreduced bipyrazine ligands for the one- and two-electron-reduction products as seen in the complexes of $[Ru(bpy)_3]^{2-n}$ and $[Ru(bpm)_3]^{2-n}$.

Introduction

The recognition of redox orbital localization within a single ligand in d^6 metal tris(diimines)[1-3] has prompted investigation into the mechanism behind the molecular symmetry lowering. One method of such an investigation involves varying the ligands around the metal center, and to that end some or all of the archetypical bipyridine (bpy) ligands in $Ru(bpy)_3^{2+}$ have been replaced with bipyrimidine (bpm) and bipyrazine (bpz) ligands. As is evident from the molecular structures for these ligands shown in Figure 1, this is equivalent to replacing with nitrogens the C–H moieties meta to the coordinating nitrogens for bipyrimidine and para to the coordinating nitrogens for bipyrazine. Because nitrogen is more electronegative than the carbon it replaces, the π orbitals would be expected to be lower in energy for the hetero ligands than for bpy, which could result in greater mixing of the lower energy redox orbitals with the metal orbitals through π backbonding. While the cyclic voltammetric data reported for the bpz complex[4-7] and the bpm complex[7-9] do indeed indicate the redox

† Present address: Department of Chemistry, Carnegie-Mellon University, Pittsburgh, PA 15213.

(1) Vlcek, A. A. *Coord. Chem. Rev.* **1982**, *43*, 39.
(2) DeArmond, M. K.; Hanck, K. W.; Wertz, D. W. *Coord. Chem. Rev.* **1985**, *64*, 65.
(3) Braterman, P. S.; Heath, G. A.; Yellowlees, L. J. *J. Chem. Soc., Dalton Trans.* **1985**, 1081.
(4) Crutchley, R. J.; Lever, A. B. P. *Inorg. Chem.* **1982**, *21*, 2276.
(5) Gonzales-Velasco, J.; Rubinstein, I.; Crutchley, R. J.; Lever, A. B. P.; Bard, A. J. *Inorg. Chem.* **1983**, *22*, 822.

0020-1669/87/1326-2754$01.50/0